

# Lateral Boundary Conditions in GungHo

Christine Johnson, Ben Shipway

## 1. Introduction

The Met Office is currently developing a next generation dynamical core for weather and climate prediction, known as **GungHo**. The model uses compatible finite-elements with finite-volume methods for the transport and is designed to be highly scalable and easily adaptable to future supercomputing architectures.

A limited-area version of the model is also being developed: a **limited area model (LAM)** runs over a smaller region, rather than the whole globe, and uses **lateral boundary conditions (LBCs)** prescribed from a driving model.

## 2. The GungHo model

Following *Melvin et al. (2019)*, the nonlinear system of Euler equations can be written as

$$R(x) = 0 \quad \text{where } x = (u, \rho, \theta, \Pi) \quad (2.1)$$

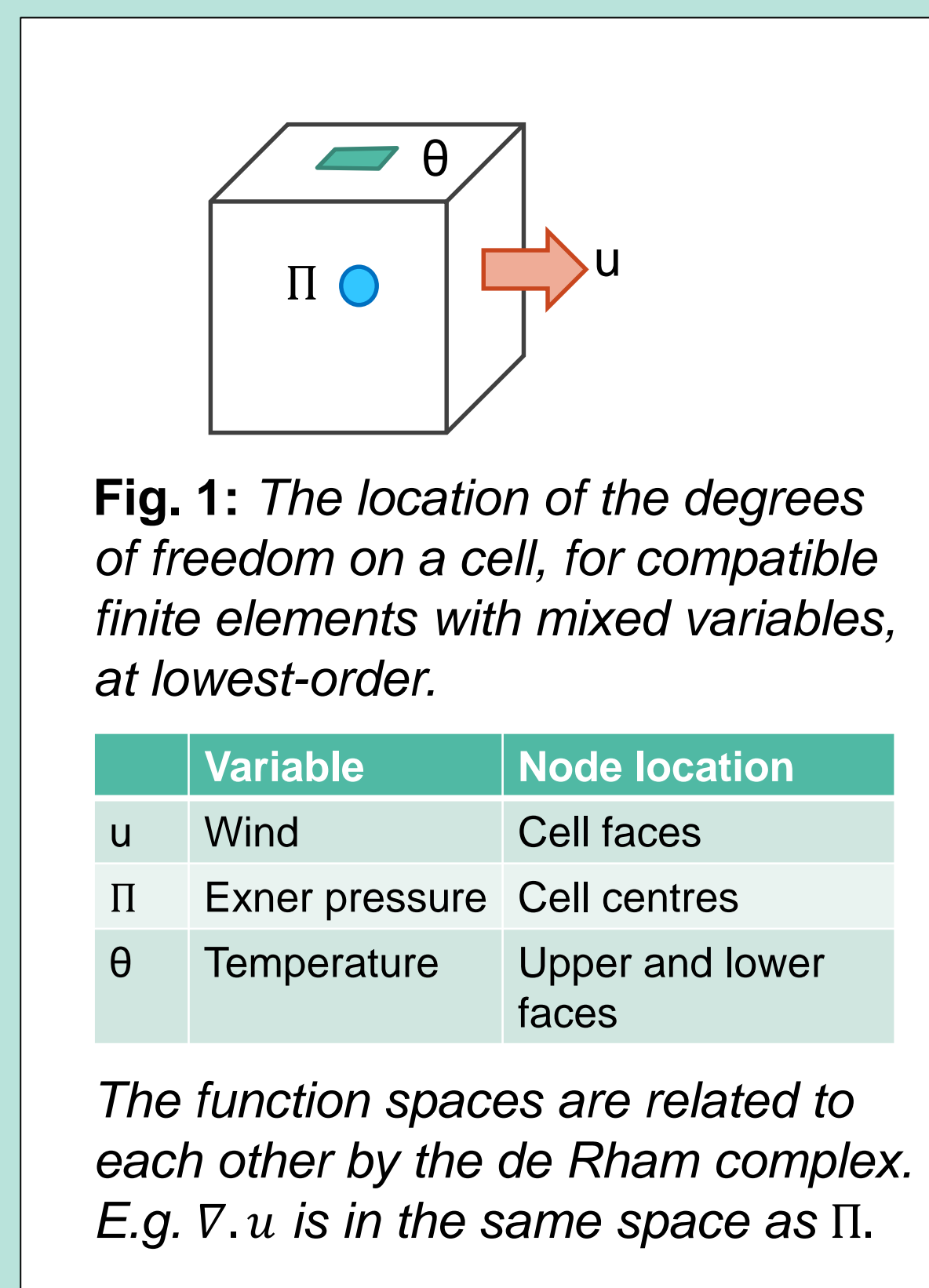
is the state vector for wind, density, potential temperature and Exner pressure. A semi-implicit time discretization is applied, so (2.1) is solved iteratively with a quasi-Newton algorithm. The state at time  $t^n$  and iteration  $k$  is given by the previous state plus an increment

$$x_{k+1}^{n+1} = x_k^{n+1} + x'_k, \quad x_0^{n+1} = x^n. \quad (2.2)$$

The mixed state increment  $x'_k$  satisfies

$$L(x^*)(x'_k) = -R(x_k^{n+1}) \quad (2.3)$$

which is solved with a Krylov solver. The linear model  $L$  approximates the Jacobian, and uses the reference profile  $x^* = x^n$ .



## 3. LBCs for the linear solver

To apply LBCs to the linear system (2.3), we split the increment  $x'_k$  into the unknown homogeneous interior,  $x'_H$  and the known boundary value,  $x'_B$ . With  $x'_k = x'_H + x'_B$ , this gives the modified system with new RHS

$$L(x^*)(x'_H) = -R(x^n) - L(x^*)(x'_B) \quad (3.1)$$

which is solved using the same Krylov solver as for the driving model.

The LBCs are specified by the difference in the wind field from the current iteration state and the driving model, on the boundary

$$x'_B = x_{driving}^{n+1} - x_k^{n+1} \quad (3.2)$$

This is specified only on the boundary, and is therefore just the wind increment field. It infers a Neumann boundary condition in the associated Helmholtz equation.

Note that in GungHo the Helmholtz equation can only be inferred in theory, and is not solved directly. This is because the mass matrix for the wind field is non-diagonal and hence difficult to invert. However, a Helmholtz equation using a mass-lumped mass matrix is used as a preconditioner, and the boundary conditions are also used in this.

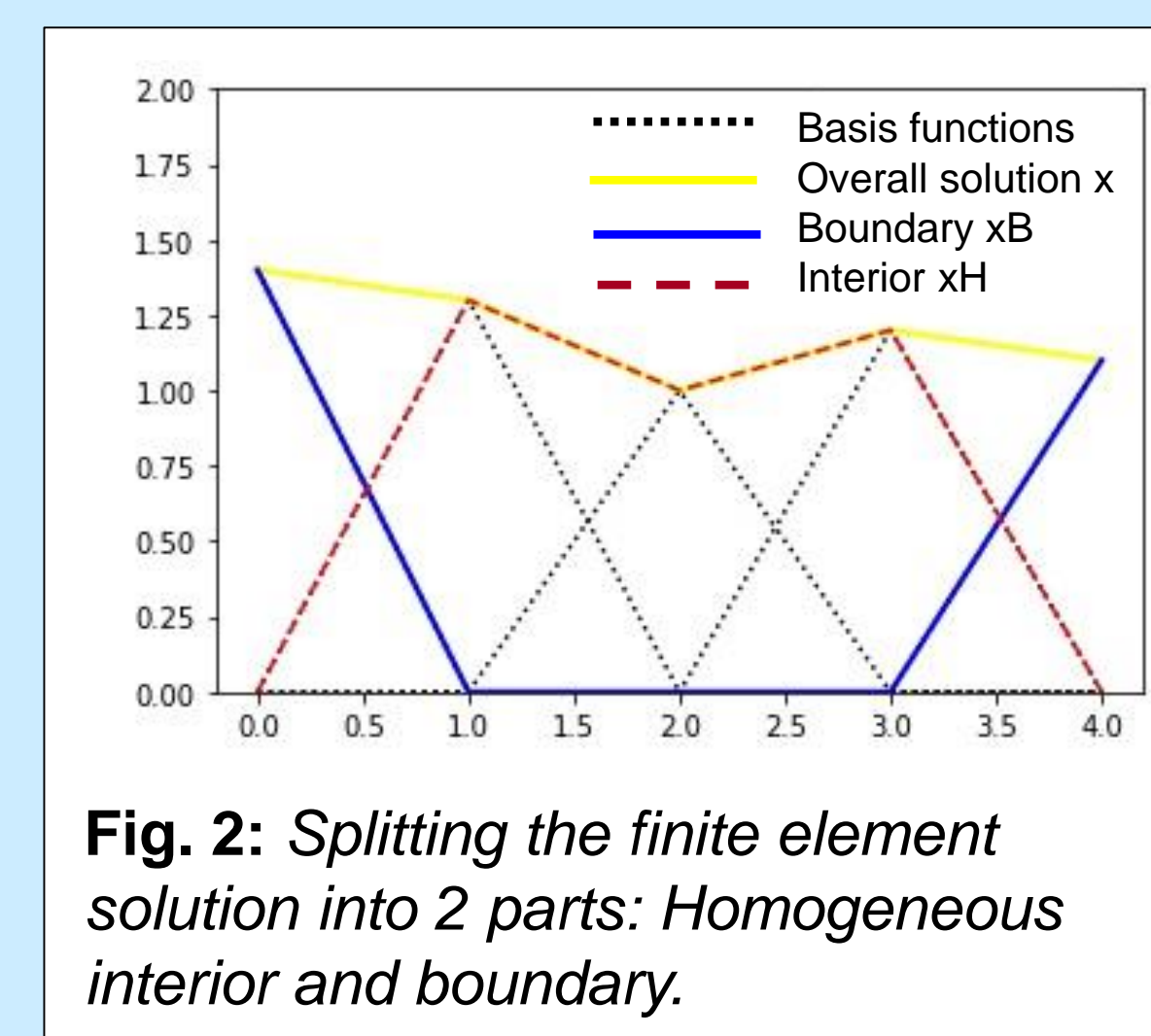


Fig. 2: Splitting the finite element solution into 2 parts: Homogeneous interior and boundary.

## 4. Boundary conditions for the inferred Helmholtz equation in a simple system

Consider the system\* for wind  $u'$  and pressure  $p'$ :

$$\begin{aligned} u' + \nabla p' &= 0 \\ p' - \nabla \cdot u' &= 0 \end{aligned} \quad (4.1)$$

Apply the boundary condition  $u'_B$  and solve in the interior,

$$\begin{aligned} u'_H + \nabla p'_H &= 0 \\ p'_H - \nabla \cdot u'_H &= \nabla \cdot u'_B. \end{aligned} \quad (4.2)$$

This can be combined to give the Helmholtz equation

$$p'_H + \nabla \cdot \nabla p'_H = \nabla \cdot u'_B. \quad (4.3)$$

\* Note that the full system has extra variables, forcings, and finite element mass matrices.

The mixed system (4.2) is therefore equivalent to solving the Helmholtz equation

$$p' - \nabla \cdot \nabla p' = 0 \quad (4.4)$$

with Neumann boundary conditions

$$\nabla p = u'_B \quad \text{normal to the boundary.} \quad (4.5)$$

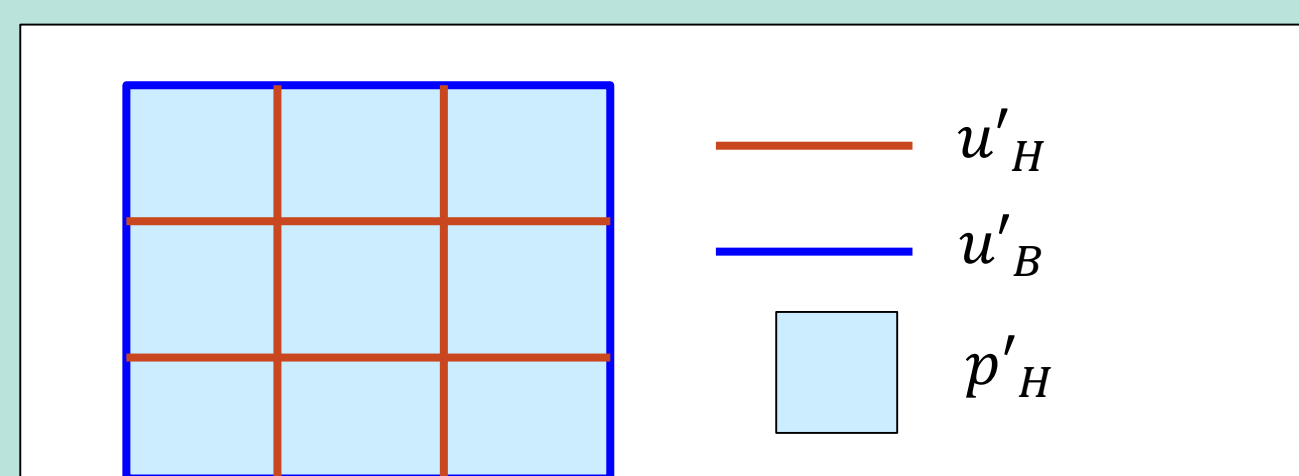


Fig. 3: The location of variables on interior faces  $u'_H$ , cells  $p'_H$ , and boundary faces  $u'_B$ .

## 5. LBCs for transport and blending

The nonlinear model contains advective terms, which also require LBCs. This is achieved in a similar way to *Davies (2014)* by specifying driving model data in a rim around the edge of the domain.

Due to differences between the LAM and driving model, the LAM solution can evolve differently to the driving model, causing mismatches at the boundaries. Therefore, on every iteration, the driving model data is blended with the LAM, near to the boundary, using weights,  $w$ ,

$$x_{lam}^{blended} = w x_{driving} + (1 - w) x_{lam}. \quad (5.1)$$

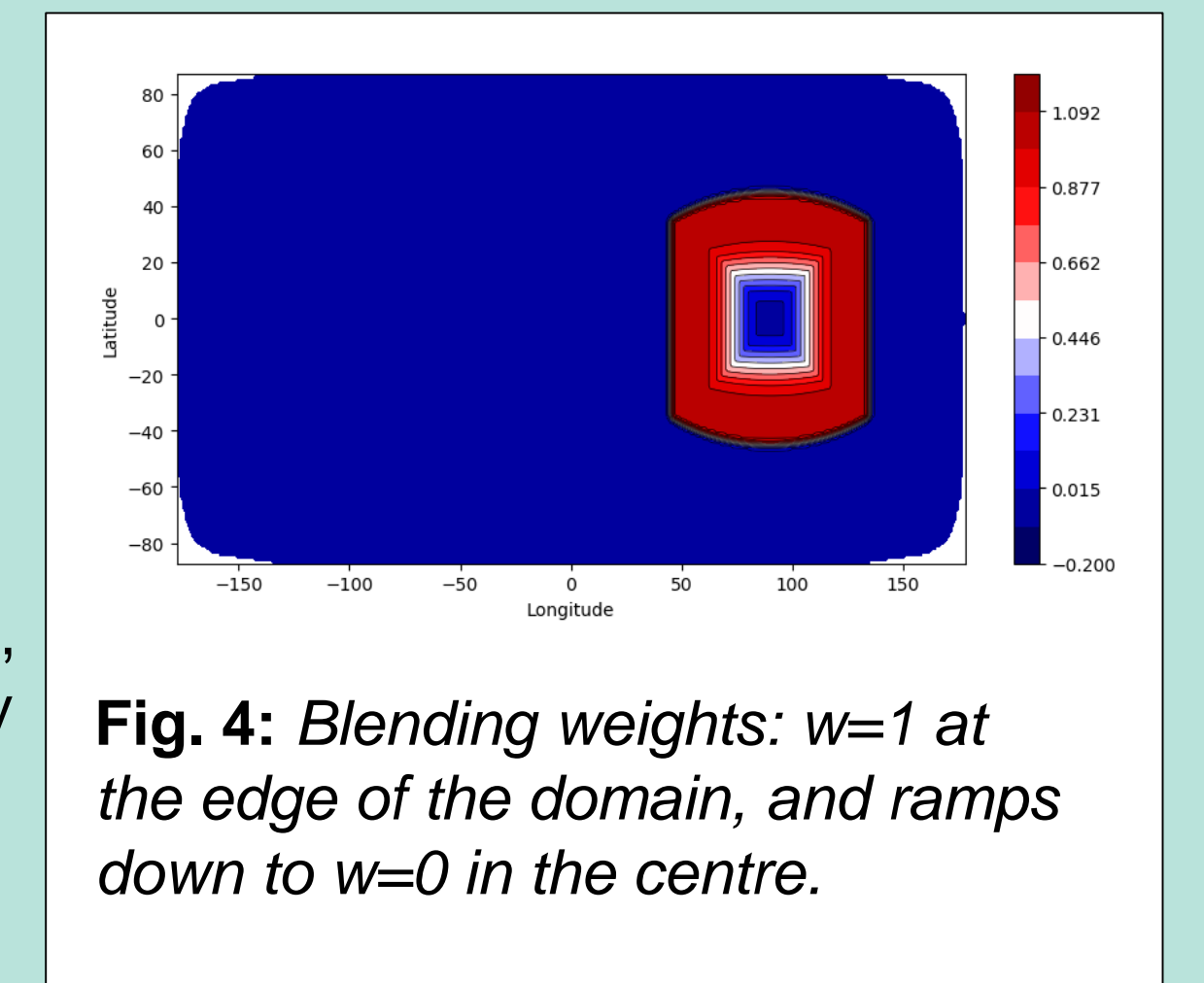


Fig. 4: Blending weights:  $w=1$  at the edge of the domain, and ramps down to  $w=0$  in the centre.

## 6. Big-brother experiment results

In operational forecasts, the LAM will run on a mesh with a different orientation and higher resolution than the driving model, and with boundary conditions interpolated in both time and space from the driving model. But for testing and development purposes, we need to isolate the impact of boundary conditions; this can be achieved using idealized experiments known as big-brother experiments.

In a big-brother experiment, both the driving model and limited area model are run using exactly the same resolution mesh, and the same model configuration. Boundary conditions are updated on every timestep. This means that, apart from rounding error from the solver, the solutions should be exactly the same.

Note that in the following experiments the LAM actually uses the full driving model mesh, due to technical reasons. It is a pseudo-LAM where the solution is only allowed to evolve in the limited area region, and boundary conditions are applied at the edge of this region.

**Straka test:** The full model uses a Cartesian, biperiodic domain. In the full model a density current is driven along the lower boundary. This is repeated in the LAM, and it then disappears at the boundary.

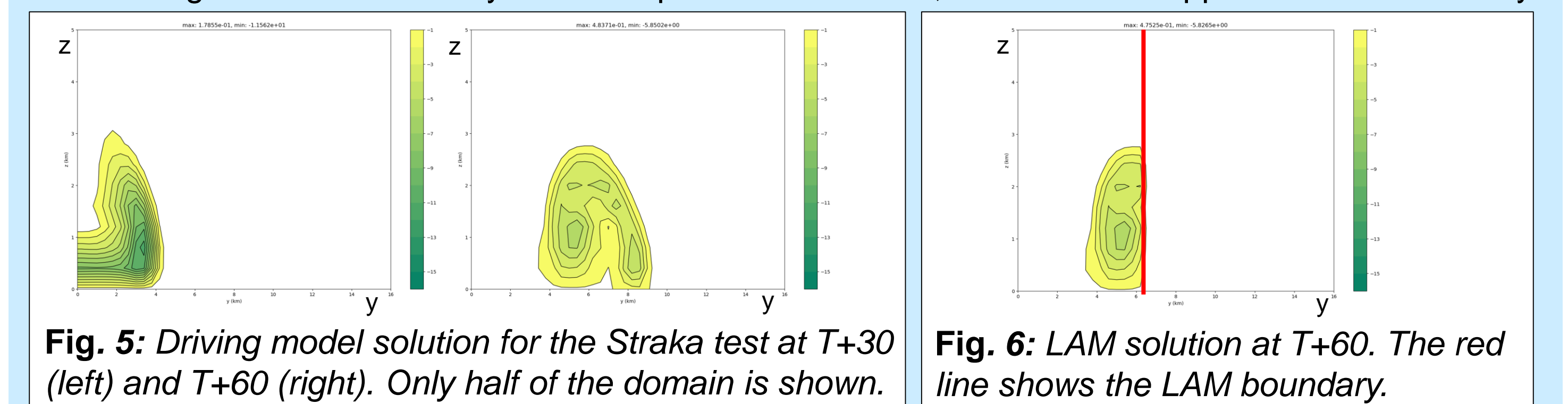


Fig. 5: Driving model solution for the Straka test at T+30 (left) and T+60 (right). Only half of the domain is shown.

Fig. 6: LAM solution at T+60. The red line shows the LAM boundary.

**Baroclinic wave test:** The full model uses a C24 cubed sphere mesh, and the limited area model region is on 1 panel of the cubed sphere.

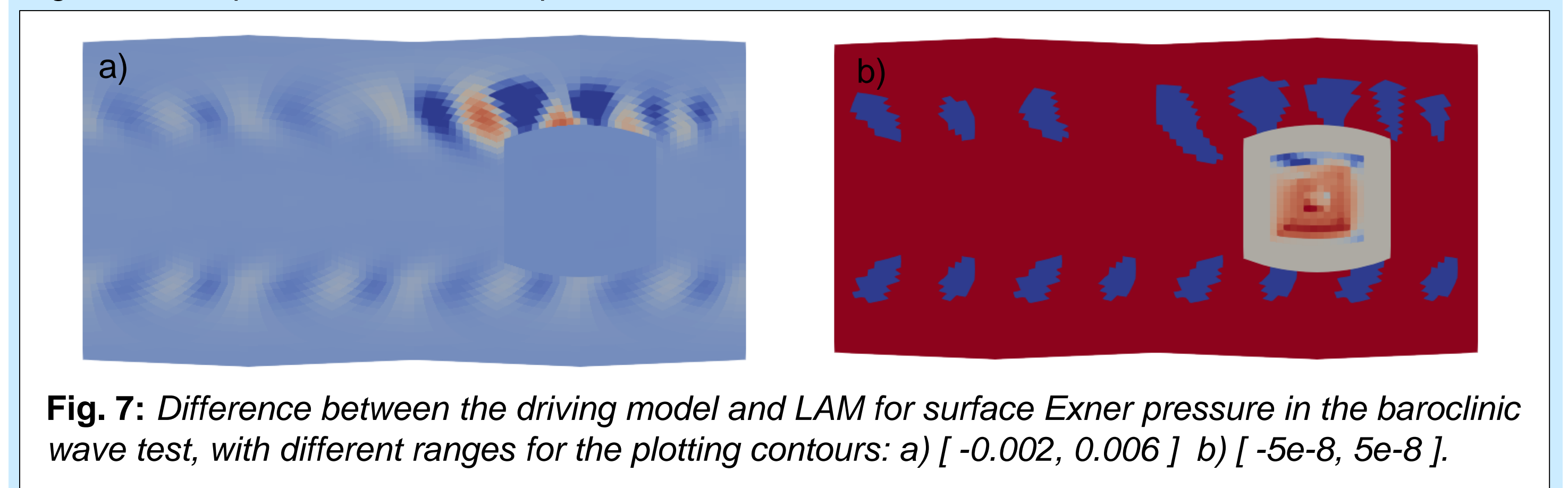


Fig. 7: Difference between the driving model and LAM for surface Exner pressure in the baroclinic wave test, with different ranges for the plotting contours: a)  $[-0.002, 0.006]$  b)  $[-5e-8, 5e-8]$ .

The difference plots show that the solution in the limited area region is almost identical for the LAM and the driving model. Fig. 7a shows that significant differences are only outside of the limited area region – where only the driving model has been allowed to evolve. In Fig. 7b the smaller plotting contour range magnifies the errors in the limited area region, showing zero difference where the blending weights are  $w=1$ , and very small differences where  $w=0$ , resulting from rounding errors.

## 7. Conclusions

- LBCs have been implemented for the GungHo model: using the wind increment in the linear solver, and blending driving model data with the LAM around the edge of the domain.
- Big-brother experiments show that the LAM solution is almost identical to the driving model solution, except for differences originating from rounding errors in the solver.
- Future work includes running the LAM on a limited area mesh, and using boundary conditions that have been reconfigured and time interpolated from a global model at a lower resolution.

## 8. References

Davies T, Lateral boundary conditions for limited area models. *Q. J. R. Meteorol. Soc.* 2014; 185–196. <https://doi.org/10.1002/qj.2127>

Melvin T, Benacchio T, Shipway B, Wood N, Thuburn J, Cotter C. A mixed finite-element, finite-volume, semi-implicit discretization for atmospheric dynamics: Cartesian geometry. *Q J R Meteorol. Soc.* 2019;1-19. <https://doi.org/10.1002/qj.3501>

